Modulation of plant chemistry by rhizosphere bacteria

Jeon, J.

Chapter 5

Effects of sulfur assimilation in *Pseudomonas fluorescens* on growth, shoot metabolome and defense of Brassica species

Je-Seung Jeon, Desalegn W. Etalo, Natalia Carreno-Quintero,
Ric De Vos, and Jos M. Raaijmakers

Manuscript submitted for publication

Abstract

Genome-wide analysis of plant growth-promoting *Pseudomonas fluorescens* strain SS101 (*Pf* SS101) combined with site-directed mutagenesis recently revealed that sulfur assimilation plays an important role in growth promotion and induced systemic resistance of the model plant Arabidopsis. Here we investigated how sulfur metabolism of *Pf* SS101 affects the shoot metabolome of Arabidopsis and of the related Brassica crop Broccoli. To this end, we treated roots of Arabidopsis and Broccoli seedlings with *Pf* SS101 or mutant 20H12 disrupted in the adenylsulfate reductase gene *cysH,* a key gene involved in sulfur assimilation and the biosynthesis of cysteine and methionine. Sulfur assimilation in *Pf* SS101 significantly affected growth of Arabidopsis but showed an adverse effect on shoot biomass of two Broccoli cultivars. In Arabidopsis, sulfur assimilation by *Pf* SS101 affected the levels of sulfurous as well as non-sulfurous metabolites in the shoot. The impact on the sulfur-containing metabolites was mainly reflected in long chain aliphatic glucosinolates. Arabidopsis treated with the *cysH* mutant showed significantly higher levels of short and medium chain aliphatic glucosinolates as compared to plants treated with wild type *Pf* SS101. Moreover, both *Pf* SS101 and *cysH* mutant treatments significantly enhanced the levels of indole metabolites such as camalexin and indole-3-acetic acid in the Arabidopsis shoot. In Broccoli, *Pf* SS101 triggered significant changes in the shoot metabolome towards defensive metabolites such as indole glucosinolates and phenylpropanoids. Furthermore, root tip treatment of two Broccoli cultivars with *Pf* SS101 significantly reduced disease severity caused by the bacterial leaf pathogen *Xanthomonas campestris* pv. armoraciae (*Xca*) but not for *Xanthomonas campestris* pv. campestris (*Xcc*). Treatment of the root tips with the *cysH* mutant only reduced disease severity in Broccoli cultivar Malibu. In conclusion, sulfur assimilation by *Pf* SS101 had a significant impact on the biosynthesis of sulfurous and non-sulfurous metabolites in the plant shoots. These changes in the host metabolome are likely associated with the observed systemic defense against bacterial infections of the leaves, but the success and magnitude thereof depend on the plant cultivar and the pathogen pathovar.

Keywords: *Pseudomonas fluorescens*; sulfur metabolism; plant growth promotion; induced systemic resistance; plant metabolomics; glucosinolates; flavonoids.

Introduction

The genus *Pseudomonas* is an abundant member of the plant microbiome, particularly of the rhizosphere. Various studies have shown that different strains of root-associated *Pseudomonas* species can promote plant growth, alter root architecture and induce systemic resistance (Vessey, 2003; Pieterse *et al.*, 2014; Etalo *et al.*, 2018). Recent studies also revealed that some root-colonizing *Pseudomonas* strains can significantly alter shoot and root chemistry. More specifically, we demonstrated that plant growth-promoting *Pseudomonas fluorescens* strain SS101 (*Pf* SS101) altered the levels of glucosinolates, coumarins, flavonoids, and camalexin in shoots and roots of Arabidopsis (van de Mortel *et al.*, 2012). Also, *P. fluorescens* strain N21.4 was shown to enhance the level of isoflavonoids in soybean (Algar *et al.*, 2014). Another interesting recent finding was that *Pseudomonas simiae* strain WCS417 induced root exudation of scopoletin, an iron-mobilizing coumarin with antimicrobial activity, suppressing the growth of fungal root pathogens but supporting root colonization by beneficial *Pseudomonas* strains (Stringlis, Ioannis A *et al.*, 2018). For most root-associated *Pseudomonas* strains, however, the specific traits that trigger phenotypic and metabolome changes in different host plants are yet unknown.

By screening a genome-wide library of approximately 7,500 random transposon mutants, we identified specific genes in *Pf* SS101 that were associated with growth promotion and induced systemic resistance in Arabidopsis (Cheng *et al.*, 2017). Twenty-one mutants were identified with a compromised ability to promote plant growth, to alter root architecture or to trigger systemic resistance against the bacterial leaf pathogen *Pseudomonas syringae* pv. tomato (Pst). Subsequent validation by site-directed mutagenesis and genetic complementation of the mutants demonstrated that the phosphogluconate dehydratase gene *edd*, the response regulator gene *colR* and the adenylsulfate reductase gene *cysH* play important roles in plant growth promotion, alteration of root architecture and induced systemic resistance (ISR) by *Pf* SS101. *CysH* is a gene involved in sulfur assimilation and the biosynthesis of the amino acids cysteine and methionine. Transcriptome analysis of Arabidopsis further revealed that biosynthetic processes associated with sulfur compounds (in particular cysteine and glucosinolates) were the most significantly enriched in seedlings treated with *Pf* SS101 as compared to the control plants and to plants treated with the *cysH* mutant (Cheng *et al*. 2017). These results indicated that *Pf* SS101 modulates sulfur metabolism in Arabidopsis confirming and extending results from Meldau *et al.* (2013) and Aziz *et al*. (2016) who attributed modulation of sulfur metabolism as a key mechanism of growth promotion and induction of lateral roots of tobacco and Arabidopsis by different *Bacillus* strains.

In the present study, we investigated the effects of sulfur metabolism (i.e. effects of the *cysH* mutation) in *Pf* SS101 on the shoot metabolome of Arabidopsis. To that end, we adopted a nontargeted metabolomics approach to assess the differences between the shoot metabolomes of Arabidopsis seedlings treated with either *Pf* SS101 or with *cysH*-mutant 20H12. Furthermore, we investigated if strain *Pf* SS101 can induce similar phenotypic and

metabolome changes in shoots of the related Brassicaceous crop plant Broccoli and if also for Broccoli these changes are associated with sulfur metabolism. The *Pf* SS101-mediated phenotypic responses investigated for two Broccoli cultivars include root and shoot growth as well as induced resistance against two pathovars of *Xanthomonas campestris*, an important bacterial leaf pathogen of Broccoli and other cruciferous crops (Monteiro *et al.*, 2005).

Materials and methods

Plant material and growth

Seeds of *Arabidopsis thaliana* Columbia (Col-0) were surface-sterilized as previously described (van de Mortel *et al.*, 2012). Seeds of the two Broccoli (*Brassica olearacea* var. italica) cultivars Coronado and Malibu were kindly provided by Bejo Seeds (Trambaan1, 1749 CZ Warmenhuizen, The Netherlands). Surface sterilization of the Broccoli seeds was performed by immersing 2 - 3 g of seeds for 30 min in 30 ml of 1% (v/v) sodium hypochlorite supplemented with 0.1% (v/v) of Tween 20 followed by 3 washes with ample sterile distilled water. For the Arabidopsis assays, sterile seeds were sown on 90-mm-diameter Petri dishes containing 20 ml half-strength Murashige and Skoog (MS) agar media, containing 0.5% sucrose (w/v) and 1.2% plant agar (w/v). For the Broccoli assays, five sterile seeds were sown on 140-mm-diameter petri dishes containing 50 ml of half-strength MS agar. The plates were then placed in a climate chamber maintained at 21°C /21°C day/night; 180 µmol light $m^{-2}s^{-1}$, 16 h light/8 h dark cycle and 70% relative humidity. After a week of Arabidopsis growth and five days of Broccoli growth, roots of each seedling were inoculated with a 2 µl of bacteria suspension (~10^9 cells ml^{-1}). After inoculation, plants were placed back in the same growth chamber until harvest.

Bacterial strains and culture conditions

Pseudomonas fluorescens strain SS101 (*Pf* SS101) was originally isolated from the wheat rhizosphere (de Souza *et al.*, 2003). *CysH*-mutant 20H12 of *Pf* SS101 was generated by site-directed mutagenesis as described by Cheng *et al*. (2017). *Pf* SS101 and mutant 20H12 were cultured in King's medium B (KB) at 25°C for 16h. Broccoli leaf pathogens *Xanthomonas campestris* pv. armoraciae (*Xca*) and *Xanthomonas campestris* pv. campestris (*Xcc*) were kindly provided by Bejo Seeds and were cultured in Luria Bertani (LB) medium (Lennox, Carl Roth) at 25°C for 16h. Bacterial cells were collected by centrifugation, washed three times with 10 mM $MgSO_{4,}$ and resuspended in 10 mM $MgSO_4$ to a final density of 10^9 cells ml^{-1} (OD_{600} = 1.0).

Disease assay for induced resistance against the leaf pathogen *Xanthomonas*

For infection, the first true leaves of the Broccoli seedlings were pierced and 2 µl (10^9 cells

ml^{-1}) of the bacterial pathogens *Xca* and *Xcc* inoculum was applied at 11 days post inoculation (dpi) of *Pf* SS101 or the *cysH* mutant to the roots. Ten days after pathogen challenge, disease severity on the shoot was assessed by determining the migration of the lesion from the inoculation spot to other parts of the shoot based on a 0-5 ordinal scale as shown in the Supplementary Material (**Figure S3**): 1 = no necrosis or migration, 2 = necrosis of the treated leaf, 3 = migration of the lesion to the leafstalk of the treated leaf, 4 = visible necrotic or water-soaked lesions of the neighboring (nontreated) leaf, and 5 = infection of the entire shoot. Severity values were converted to 0 to 100 Disease severity index (DSI) according to the following equation used by (Vieira *et al.*, 2012). DSI (%) = ∑ (scores of all plants)/ [Maximum disease score x (total number of plants)] x 100. Next to this disease severity assessment, treated Broccoli shoots were collected, ground in a sterile mortar and suspended in 50 mL Falcon tube to measure its biomass. Samples were then vortexed for 60 s in 10 mM MgSO4, sonicated for 60 s, and again vortexed for 15 s. The suspension was serially dilution plated onto KB agar plates containing 100 µg ml^{-1} delvocid (DSM) to inhibit fungal growth and incubated for 3 days at 25 °C. Colonies with the typical phenotype of *Xca* and *Xcc* were counted and expressed as colony-forming units (cfu) mg^{-1} of shoot fresh weight.

Plant metabolite analysis

Sample preparation

Shoots of Arabidopsis and Broccoli were harvested at 11 days after root treatment with buffer (control), *Pf* SS101 or with mutant 20H12. For each plant species/cultivar X rhizobacteria combination, 4 biological replicates were used with ten Arabidopsis and five Broccoli seedlings per replicate. In brief, shoots were snap frozen in liquid nitrogen and ground to fine powder under continuous cooling and kept at -80 °C until further use. To extract semi-polar secondary metabolites, 300 µL of 99.89% methanol containing 0.13% (v/v) formic acid was added to 100 mg plant material in 2 ml round bottom Eppendorf tubes, and sonicated for 15 min followed by centrifugation for 15 min at 20,000 x *g*. The supernatants were transferred to 96-well filter plates (AcroPrepTM, 350 µl, 0.45µm, PALL), vacuum filtrated to the 96-deep-well autosampler plates (Waters) using a Genesis Workstation (Tecan Systems).

Metabolite analysis

An UltiMate 3000 U-HPLC system (Dionex) was employed to create a 45-minutes linear gradient of 5-35% (v/v) acetonitrile in 0.1% (v/v) formic acid (FA) in water at a flow rate of 0.19 ml per min. 5 µl of each extract was injected and compounds were separated on a Luna C18 column (2.0 x 150 mm, 3µm; Phenomenex) maintained at 40 °C (De Vos *et al.*, 2007). The detection of compounds eluting from the column was carried out with a Q-Exactive Plus Orbitrap FTMS mass spectrometer (Thermo Scientific). Full scan MS data were generated with electrospray in switching positive/negative ionization mode at a mass resolution of

35,000 (FWHM at m/z 200) in a range of m/z 95-1350. Subsequent MS/MS experiments for identification of selected metabolites were performed with separate positive or negative electrospray ionization at a normalized collision energy of 27 and a mass resolution of 17,500. The ionization voltage was optimized at 3.5 kV for positive mode and 2.5 kV for negative mode; capillary temperature was set at 250 °C; the auxiliary gas heater temperature was set to 220 °C; sheath gas, auxiliary gas and the sweep gas flow were optimized at 36, 10 and 1 arbitrary units, respectively. Automatic gain control was set a 3e6 and the injection time at 100 ms. External mass calibration with formic acid clusters was performed in both positive and negative ionization modes before each sample series.

LC-MS data processing and analysis

Peak picking, baseline correction, and mass signal alignment of the LC-MS data were performed using Metalign software (Lommen, 2009). The mass features were considered as a signal if they were detected in at least 3 biological replicates of a treatment with a signal intensity 3 times higher than the background noise value. Then, mass features originating from the same metabolites were clustered based on retention window and their correlation across all measured samples, using MSClust software (Tikunov *et al.*, 2012). After this, so-called centrotypes representing reconstructed putative metabolites mass spectra were selected, of which relative abundance was represented by the Measured Ion Count (MIC), which is the sum of the ion count values (corrected by their membership) for all measured cluster ions in a given sample. ANOVA with Benjamini–Hochberg false discovery rate (BH-FDR) correction ($P < 0.05$) and fold changes more or less than 2.0 were applied to identify mass signals that were significantly changed in bacteria-treated to control samples. Then, the bootstrapping analysis we performed to weed out duplicate signals within each mass mode and between two mass modes (positive and negative). Data transformation and scaling were performed in GeneMaths XT 1.6 (www.applied-maths.com). Transformed and scaled values were used for hierarchical cluster analysis using Pearson's correlation coefficient and Unweighted Pair Group Method with Arithmetic Mean (UPGMA).

Metabolites annotation of MS signals was carried out based on selection of pseudomolecule ions from the masses in the MSClust-reconstructed metabolites, first by matching their accurate masses plus retention times to previously reported metabolites present in Arabidopsis and Broccoli on the same LC-MS system and similar chromatographic conditions. Second, if compounds were not yet present in this experimentally obtained dedicated database, KEGG and HMDB databases basis MS/MS annotation that were mounted on MAGMa online tool (Ridder *et al.*, 2013) were primarily applied with a maximum deviation of observed mass from calculated of 5 ppm. In addition, some annotations were complemented by the aid of other publicly available compound libraries, including PubChem (https://pubchem.ncbi.nlm.nih.gov/) and Metlin (http:// metlin.scripps.edu/).

Statistical analysis

Changes in shoot biomass and pathogen incidence between treatments were analyzed with R Studio software (Version 3.6.1). The data for plant shoot and root biomass were statistically analyzed by two-way analysis of variance (ANOVA). A Tukey-HSD test was used to separate group mean values when the ANOVA was significant at $P < 0.05$. For the disease severity data, beta regression analysis was employed to examine the interaction effect of two independent variables (Rhizobacteria and Broccoli cultivars) on disease severity of the two bacterial pathogens using ("betareg") package in R.

Results

Role of the *cysH* gene of *P. fluorescens* SS101 in plant growth promotion

Treatment of Arabidopsis roots with *Pf* SS101 led to a significant increase in total plant biomass (62.8% ± 4.6) (**Fig 1b1**). Inoculation with *cysH*-mutant 20H12 also increased plant biomass (35.1% ± 4.8) relative to the untreated control, but the magnitude of the growth promotion was significantly less than that observed for wild type *Pf* SS101. *Pf* SS101 significantly increased root biomass (44.5% ± 0.6) whereas *cysH*-mutant 20H12 did not affect root biomass and did not have major effects on root architecture as observed for wild type *Pf* SS101 which reduces the length of the primary root and enhances lateral root formation (**Fig 1a** and **1b3**).

For the two Broccoli cultivars, the impact of *Pf* SS101 and mutant 20H12 on plant growth was different from that observed for Arabidopsis. In Broccoli, there was a significant interaction effect between the Broccoli cultivars and the rhizobacteria (wild type/mutant) for the shoot, root and total biomass (Supplementary **Table S1**). Overall, the total biomass of both Broccoli cultivars upon root treatment with *Pf* SS101 showed no significant changes relative to the non-treated controls. However, *Pf* SS101 significantly affected biomass allocation to shoot and roots with significant reductions of the shoot biomass in both cultivars (-22.1% ± 2.6 and -15.6% ± 5.1 in Coronado and Malibu, respectively) and significant increases in root biomass (71.7% ± 14.2 in Coronado and 29.0% ± 5.0 in Malibu) (**Fig 1**). Mutant 20H12 significantly enhanced total biomass of Broccoli cultivar Malibu but not of cultivar Coronado. The change in biomass allocation to shoot and roots was not as apparent for mutant 20H12 as it was for wild type *Pf* SS101. Compared to wild type *Pf* SS101, however, the total biomass of both Broccoli cultivars was significantly higher in the 20H12 treatment. Collectively these results suggest that sulfur assimilation in *Pf* SS101 contributes positively to growth promotion of Arabidopsis, whereas for Broccoli it has a neutral to negative effect on growth depending on the cultivar.

To determine if these differential effects on plant biomass were associated with differences

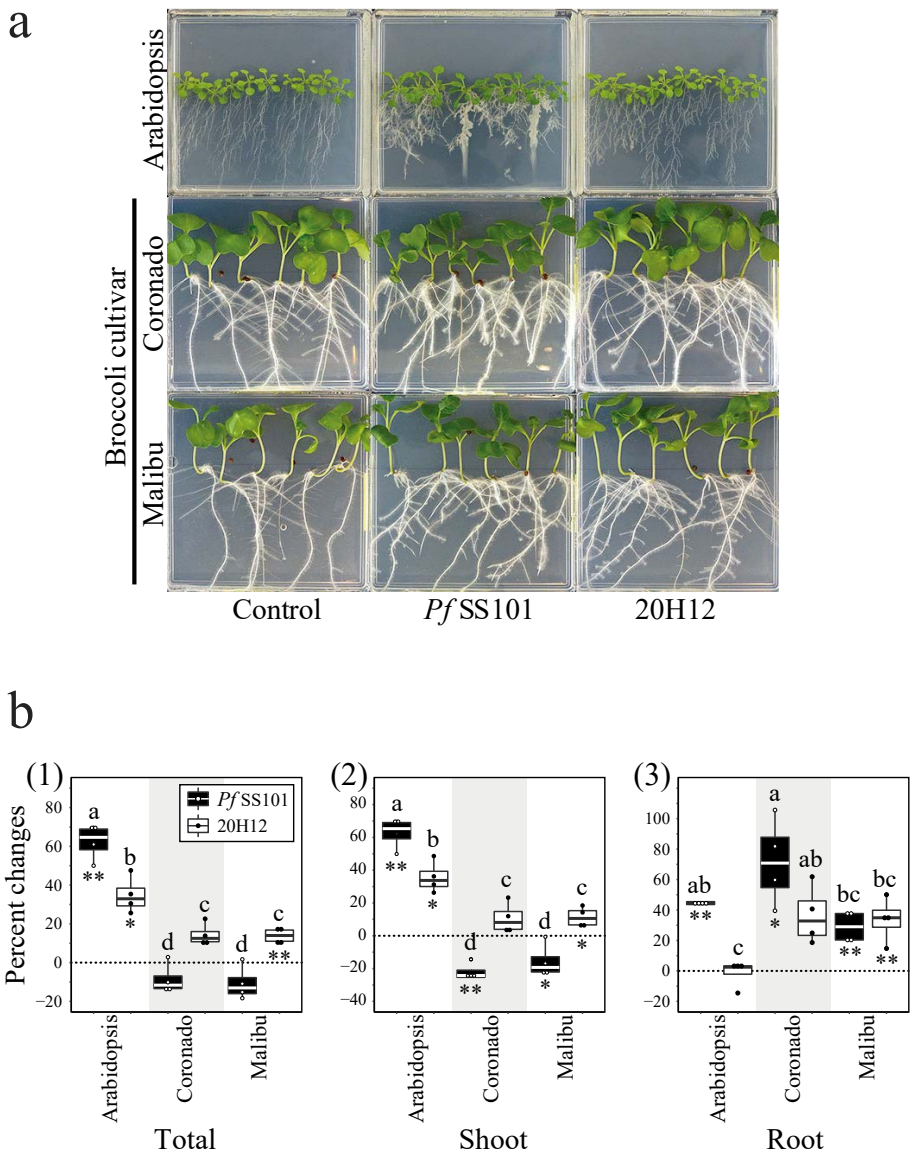

Fig 1. Phenotypic changes in Arabidopsis and Broccoli seedlings upon root treatment by *P. fluorescens* SS101 or its *cysH* mutant 20H12. Photographs of MS agar plates with Arabidopsis, and two Broccoli cultivars (Coronado, Malibu) treated on the root tip with *Pf* SS101 (wild type) or its *cysH* mutant (20H12) (**a**). Percent change in fresh biomass of shoot and root of plants treated with rhizobacteria when compared to untreated plants (11dpi) (**b**). Means of percent changes in biomass with a different letter are significantly different among treatments according to two-way ANOVA (Tukey, $P<0.05$). Asterisks denote statistically significant differences (two-tailed Student's t test): * $P < 0.05$; ** $P < 0.01$ of rhizobacteria treated plants when compared to the controls. For each plant species, four independent biological replicates were used with 10 seedlings of Arabidopsis and 5 of Broccoli per biological replicate. *Pf* SS101: *Pseudomonas fluorescens* SS101, 20H12: *cysH* gene mutant of *Pf* SS101.

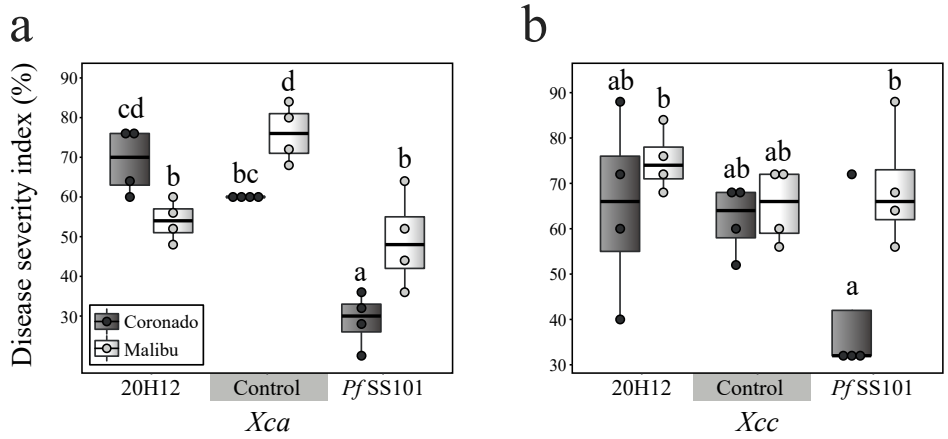

Fig 2. Rhizobacteria-mediated resistance in two Broccoli cultivars, Coronado and Malibu, against the bacterial leaf pathogens *Xanthomonas campestris*: *Xanthomonas campestris* pv. armoraciae (*Xc*a) (**a**) and *Xanthomonas campestris* pv. campestris (*Xcc*) (**b**). Prior to pathogen inoculation on the leaves, roots of each Broccoli cultivar were treated with *P. fluorescens* SS101 or its *cysH*-mutant 20H12 and incubated for 11 days. For the disease severity caused by *Xca* or *Xcc*, Broccoli seedlings from four biological replicates were individually scored (n = 20). Disease severity was scored on a scale from 0-5, where 1 = no necrosis or migration, 2 = full infection of the treated leaf, 3 = migration of the infection to the leafstalk of the treated leaf, 4 = infection of the neighboring leaf, and 5 = infection of the entire seedling (see supplementary material **Fig S3**). Different letters above bars indicate statistically significant differences based on beta regression analysis followed by Tukey test ($P < 0.05$).

in root colonization, rhizosphere population densities of *Pf* SS101 and *cysH*-mutant 20H12 were assessed at 11 dpi. The results showed that for Arabidopsis and for the two Broccoli cultivars, mutant 20H12 generally established up to 10-fold higher rhizosphere population densities than *Pf* SS101: 20H12 established population densities ranging from 2.0 ± 0.1 x 10^6 to 5.3 ± 0.3 x 10^6 CFU mg^{-1} whereas densities of *Pf* SS101 ranged from 2.2 ± 0.3 x 10^5 to 9.9 ± 0.5 x 10^5 CFU mg^{-1} (Supplementary **Table S2**). These results indicate that the *cysH* gene adversely affects root colonization of Arabidopsis and Broccoli by *Pf* SS101. When we plotted the different rhizobacterial densities against the plant biomass changes relative to the non-treated controls (Supplementary **Fig S2**), no overall consistent pattern was found: higher rhizobacterial population densities were associated with positive, negative or no changes in shoot and root biomass of the treated plants.

Role of the *cysH* gene of *P. fluorescens* SS101 in induced resistance

For the two Broccoli cultivars, we also looked into the effect of root inoculation with *Pf* SS101 or the *cysH*-mutant 20H12 on infection of the leaves by two pathovars of the bacterial leaf pathogen *Xanthomonas campestris*. Broccoli cultivar Coronado treated with *Pf* SS101 and challenged by *Xanthomonas campestris* pv. armoraciae (*Xca*) showed significant reduction in disease severity, whereas root treatment with mutant 20H12 was not effective

(**Fig 2a**). By contrast, both *Pf* SS101 and mutant 20H12 induced resistance in cultivar Malibu against *Xca* (**Fig 2**). However, *Pf* SS101 and mutant 20H12 had no significant impact on *Xcc* severity for both Broccoli cultivars (**Fig 2B**). The results further showed that the qualitative disease severity index correlated, in most cases, with the cell density of the two *Xanthomonas* pathovars, i.e. a higher disease severity index corresponded to a higher cell density of the *Xc* pathovars in the leaves (Supplementary **Fig S4**). An exception was the density of *Xcc* in leaves of *Pf* SS101-treated Malibu seedlings where a 50-fold reduction of the *Xcc* density in the leaves relative to the nontreated control was not accompanied by a lower disease severity (Supplementary **Fig S4**).

Effect of *P. fluorescens* SS101 and the *cysH* gene on the plant metabolome

Untargeted metabolome analysis was employed to investigate the impact of the *cysH* gene mutation of *Pf* SS101 on changes in the shoot secondary metabolome and to identify potential associations with the phenotypic changes induced by these rhizobacteria as descirbed above. The shoot metabolites that were significantly altered (fold change (FC) >2, $p < 0.05$ in ANOVA (Benjamini and Hochberg)) upon root treatment by *Pf* SS101 or its *cysH*-mutant 20H12 were used for principal component analysis (PCA) and hierarchical cluster analysis (HCA) for Arabidopsis and Broccoli.

Arabidopsis

From the total of 725 metabolites detected in Arabidopsis shoots in positive or negative ionization mode, 128 (18%) metabolites were significantly different between the treatments. Abundance and fold changes of each plant metabolite are shown in Supplementary Material, **Table S5**. PCA of the metabolites revealed a clear discrimination between treatments with the first three principal components explaining 90.3% of the total variance (**Fig 3a**). The first principal component (PC1) accounted for 58.3% of the total variance and associated with metabolites that showed greater depletion or accumulation in plants treated with *Pf* SS101 and 20H12 when compared to the control (**Fig 3b**, clusters **1-2** (depleted) and clusters **4-5 (**accumulated)). Metabolites in cluster **1** showed significant depletion in plants treated with *Pf* SS101 and include the short chain (C-4) isoleucine-derived aliphatic 2-methylbutyl glucosinolate (glucocleomin), amino acids and derivatives such as arginine and N-acetyl-L-tyrosine, and fattyl acyl glycosides such as (R)-pantothenic acid 4'-O-b-D-glucoside. Cluster **2** comprises metabolites that were depleted in plants treated with both *Pf* SS101 and the mutant 20H12, and the depletion was more pronounced on plants treated with *Pf* SS101. Some of the identified metabolites in this cluster include an amino acid and derivatives such as glutamine and N-(1-deoxy-1-fructosyl)proline, 5-oxoproline, fatty acyl glycosides and a hydroxycinnamic acid O-feruloylquinic acid. Metabolites that were increased by the *Pf* SS101 treatment are shown in Cluster **4** and include a long chain (C-8) aliphatic glucosinolate 8-methylthiooctyl glucosinolate, a hydroxycinnamic acid glucuronide sinapinic acid-O-

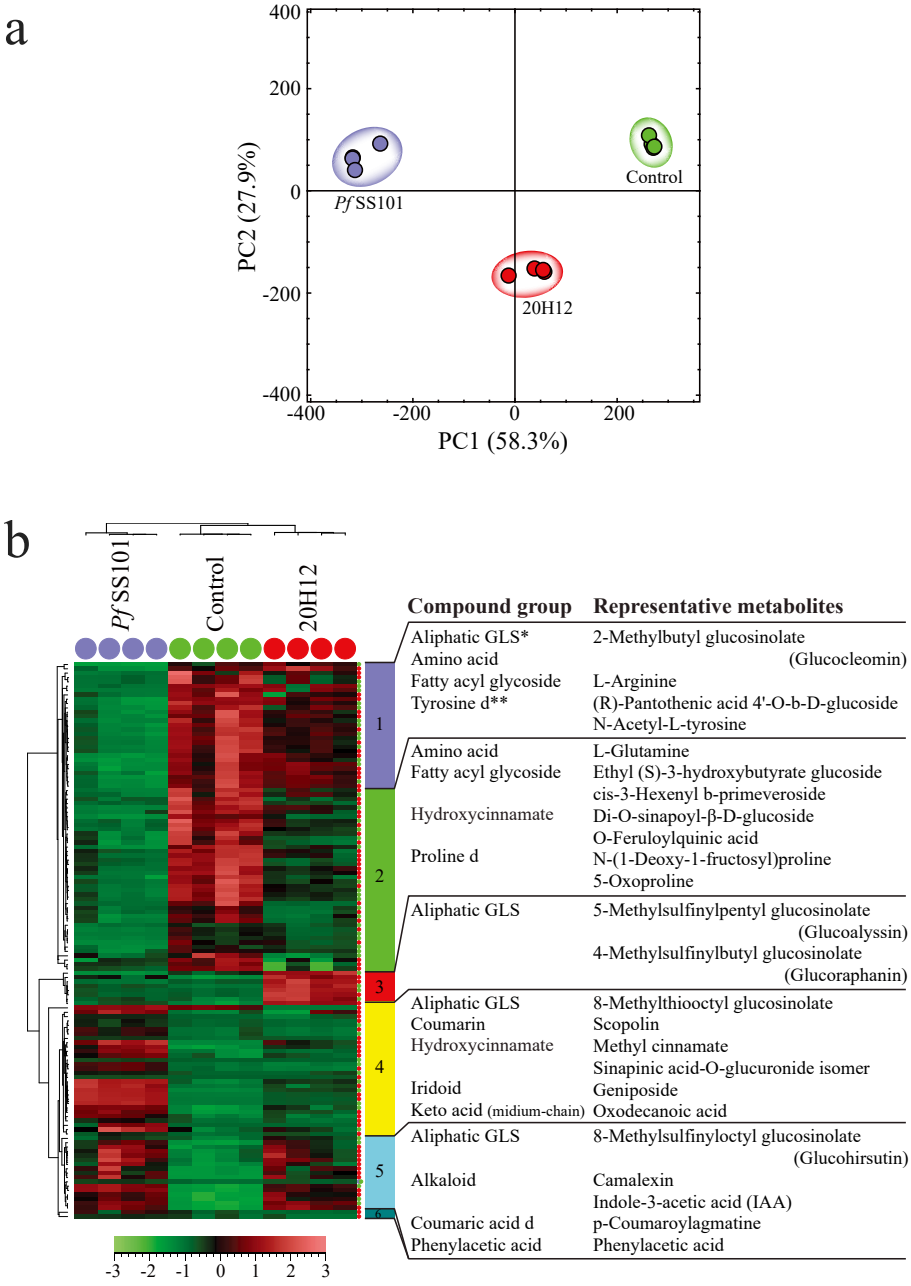

Fig 3. Metabolome changes in Arabidopsis shoots upon root treatment by *P. fluorescens* SS101 or its *cysH* mutant 20H12. Shown are the results of the principal component analysis (PCA) (**a**) and hierarchical cluster analysis (HCA) (**b**) based on differentially regulated semi-polar metabolites. In the HCA, various metabolite clusters are indicated by different colors and when none of the metabolites in a given cluster was annotated, the cluster number was omitted (Clusters 3, 5, and 10 in **Fig b**). * GLS=glucosinolate. ** d=derivative.

glucuronide, a medium chained keto acid oxodecanoic acid and the coumarin scopolin (see cluster **4**). Cluster **5** represents metabolites that were enhanced in both *Pf* SS101 and 20H12 treatments and include a long chain (C-8) aliphatic glucosinolate 8-methylsulfinyloctyl glucosinolate (glucohirsutin), a hydroxycinnamic acid amide coumaroylagmatine, and stress-associated alkaloids such as camalexin (20.5-fold up in *Pf* SS101 and 17.3-fold up in 20H12) and indole-3-acetic acid (IAA) (8.4-fold in *Pf* SS101 and 6.9-fold in 20H12). The second principal component (PC2) explained 27.9% of the total variance and includes metabolites accumulated only in the 20H12 treatment (Cluster **3**). Here, 4-methylsulfinylbutyl glucosinolate (glucoraphanin) and 5-methylsulfinylpentyl glucosinolate (glucoalyssin), middle chained (C-4 and C-5, respectively) aliphatic glucosinolate, displayed 20H12-specific accumulation.

In conclusion, the most prominent similarities in shoot metabolome changes induced in Arabidopsis shoots by *Pf* SS101 and mutant 20H12 are enhanced levels of the plant growth hormone IAA and the stress- associated alkaloid camalexin. The most prominent differences in shoot metabolome affected by the *cysH* mutation involve medium chain keto acid and the long chain (C-8) aliphatic glucosinolate 8-methylthiooctyl glucosinolate (enhanced in the *Pf* SS101 treatment to greater level) and the middle chain (C-4 and C-5) aliphatic glucosinolates 4-methylsulfinylbutyl glucosinolate and 5-methylsulfinylpentyl glucosinolate (enhanced in the 20H12 treatment to greater level).

Broccoli

The *cysH* mutation in *Pf* SS101 also had substantial impact on Broccoli shoot metabolism (**Fig 4**). Detailed information about abundance and fold change of each metabolite is shown in Supplementary Material, **Table S6**. From the total of 1908 metabolites that were detected in the Broccoli shoot samples, 830 (44%) metabolites were significantly different between the *Pf* SS101 and 20H12 treatments. In PCA, the first three PCs explained 73.7% of the total variation. The first PC explained 33.9% of the total variation and corresponds to Broccoli metabolites that were enhanced or reduced in plants treated with *Pf* SS101 and the mutant 20H12. The magnitude of the alteration of these metabolites was greater in *Pf* SS101 treatment (i.e. cluster **5**: 307 metabolites; cluster **1**: 55 metabolites). Cluster **5**, the largest cluster of *Pf* SS101-enhanced metabolites, comprised metabolites associated with plant defense-related phenylpropanoid biosynthesis such as the flavonoids kaempferol-di/tri-(feruloyl/ caffeoyl/ coumaroyl) glycosides, quercetin-tri-coumaroyl glycoside, rutin, the hydroxycinnamates caffeic acid, ferulic acid, feruloylquinic acid, sinapic acid, chlorogenic acid, neocuscutoside C, and their derivatives, and resveratrol sulfoglucoside. In addition, some phenolic glucosides including ginnalin B, hydroxybenzaldehyde diglycoside, hydrojuglone glucoside, as well as antioxidant butenolides such as ascorbic acid (vitamin C) and dehydroascorbic acid also belonged to this metabolite cluster that was accumulated in the *Pf* SS101 treatment. Among the identified glucosinolates in cluster 5, the indole glucosinolate glucobrassicin and its

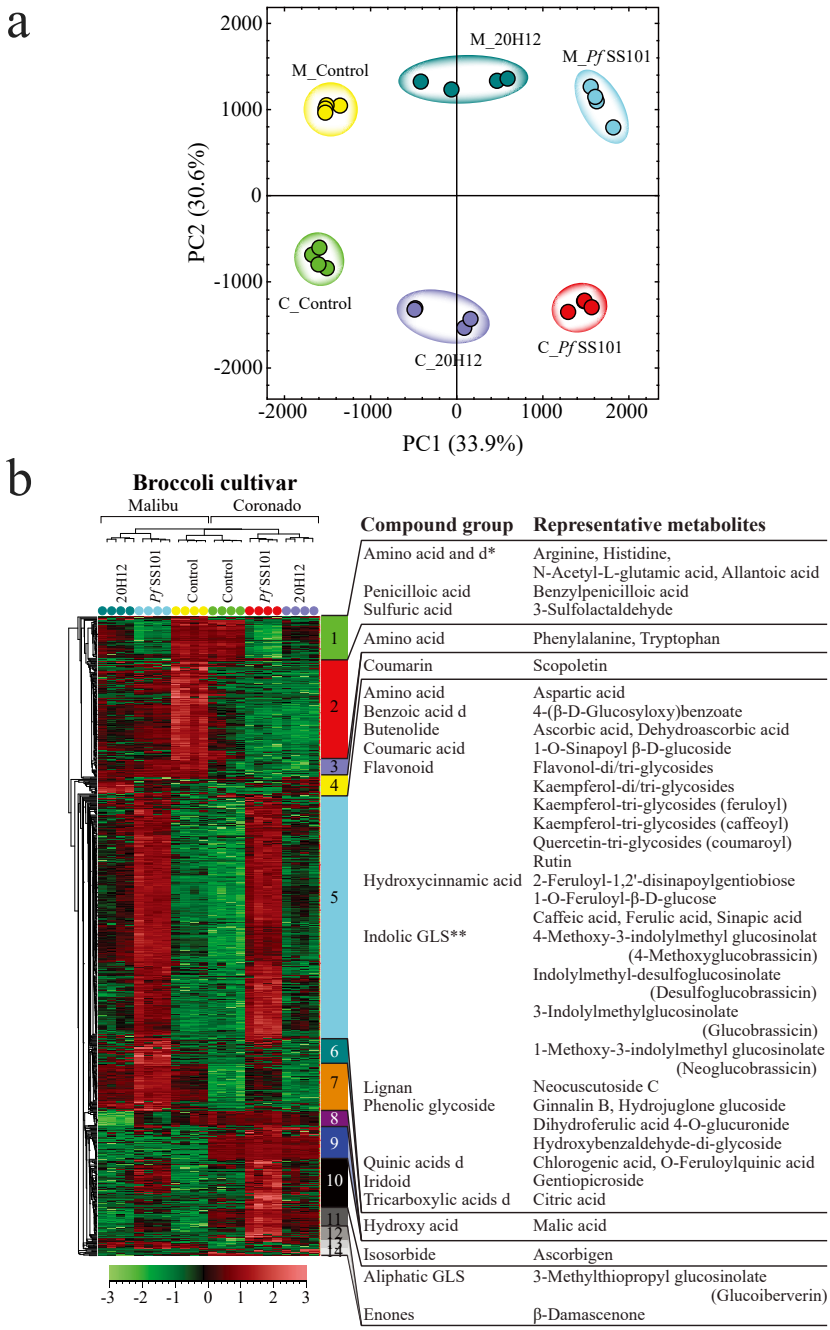

Fig 4. Metabolome changes in the shoots of two Broccoli cultivars, Coronado and Malibu upon root treatment by *P. fluorescens* SS101 or its *cysH* mutant 20H12. Shown are the results of the PCA (**a**) and HCA (**b**) based on differentially regulated semi-polar metabolites. In the HCA, various metabolite clusters are indicated by different colors; when none of the metabolites in a given cluster was annotated, the cluster number was omitted (Clusters 3, 6, 8, 9, 12, 13 and 14 in **Fig b**). * GLS=glucosinolate. ** d=derivative.

derivatives showed significant increases in the *Pf* SS101 treatment. Cluster **1** encompasses metabolites that were reduced in the *Pf* SS101 treatment and include some amino acids and derivatives, allantoic acid, benzylpenicilloic acid, as well as 3-sulfolactaldehyde. PC2 explained 30.6% of the total variation and was associated with metabolites that were intrinsically different in abundance between the two Broccoli cultivars (Clusters **2** and **7** (high in Malibu) and clusters **9** and **11** (high in Coronado). Furthermore, metabolites clusters **7**, **9** and **11** showed higher accumulation in plants treated with *Pf* SS101 when compared to the mutant 20H12. Metabolites that decreased in both Broccoli cultivars were grouped together in cluster **2** and encompassed phenylalanine and tryptophan, the building blocks for phenylpropanoid and indolic glucosinolate biosynthesis, respectively. In addition, malic acid was most abundant in Malibu (cluster **7**) while the level of the aliphatic glucosinolate glucoiberverin was much higher in Coronado (cluster **11**). The third PC explained 9.2% of the total variation and was associated with metabolites that were accumulated (cluster **4**) in both Broccoli cultivars or decreased in Malibu (cluster **8**) in plants treated with 20H12. In summary, the *cysH* mutation in *Pf* SS101 enhanced metabolites in Broccoli shoots that are associated with flavonoid, hydroxycinnamate, and indolic glucosinolate biosynthesis.

Discussion and conclusions

We previously showed that the rhizobacterium *Pf* SS101 promoted growth and altered root architecture of Arabidopsis, induced systemic resistance (ISR) and enhanced glucosinolate levels in roots and shoots (Van de Mortel *et al*. 2012). By screening a genome-wide mutant library of *Pf* SS101, we then identified the adenylsulfate reductase gene *cysH* as one of the key genes associated with growth promotion and ISR (Cheng *et al*., 2017). *CysH* is involved in sulfur assimilation and the biosynthesis of cysteine and methionine. Results from Cheng *et al*. (2017) further showed that addition of cysteine to the growth medium induced lateral root formation in Arabidopsis in a concentration dependent manner and triggered ISR against the bacterial leaf pathogen *Pseudomonas syringae.* Cysteine can enter into the glucosinolate biosynthesis pathway of plants by different routes including i) direct donation of reduced sulfur to glucosinolate biosynthesis, ii) incorporation of cysteine into methionine that, through a series of side chain elongation, S-glycosylation and other secondary modifications, ends up in the glucosinolate pool, and iii) conjugation of cysteine, glutamate and glycine to form glutathione (GSH) (Meister, 1995) which in turn acts as a sulfur donor for glucosinolate biosynthesis (Geu-Flores *et al.*, 2011). The results of our study confirmed that methionine-derived glucosinolate levels were increased in shoots of Arabidopsis upon root treatment with *Pf* SS101 and further showed higher levels of the long chain (C-8) aliphatic glucosinolates i.e. 8-methylthiooctyl glucosinolate and glucohirsutin. In leaves of Arabidopsis seedlings treated with the *cysH* mutant, the levels of long chain (C-8) aliphatic glucosinolates were lower and, instead, we observed higher levels of the C-4 and C-5 short chain aliphatic glucosinolates 4-methylsulfinylbutyl glucosinolate and 5-methylsulfinylpentyl glucosinolate,

respectively. The isoleucine-derived short chain (C-4) aliphatic glucosinolate 2-methylbutyl glucosinolate showed significant reduction in plants treated with *Pf* SS101. In Arabidopsis, side chain elongation of aliphatic glucosinolates is catalyzed by the MAM1/MAM3 proteins which condense 2-oxo acids and acetyl-CoA to extend the alkane C chain (Textor *et al.*, 2004; Textor *et al.*, 2007). Oxodecanoic acid that could be a potential substrate for chain elongation also showed greater accumulation in plants treated with *Pf* SS101. Interestingly, transcriptome analysis from our previous study also revealed that plants treated with *Pf* SS101 showed significantly higher expression of both MAM1 and MAM3 genes when compared to plants treated with mutant 20H12 or untreated plants (Cheng *et al.*, 2017). Collectively these results indicate that the *cysH* gene of *Pf* SS101 contributes to chain elongation of aliphatic glucosinolates in leaves of Arabidopsis.

For Broccoli, however, sulfur metabolism of *Pf* SS101 appeared to adversely affect shoot biomass as root treatment with the *cysH* mutant resulted in higher total biomass for both cultivars than observed for wild type *Pf* SS101. Overall, the total biomass of both Broccoli cultivars upon root treatment with *Pf* SS101 showed no significant changes relative to the non-treated controls, but *Pf* SS101 significantly affected biomass allocation to shoot and roots with significant reductions of the shoot biomass in both cultivars and significant increases in root biomass. Mutant 20H12 significantly enhanced total biomass of Broccoli cultivar Malibu but not of cultivar Coronado. The change in biomass allocation to shoot and roots was not as apparent for mutant 20H12 as it was for wild type *Pf* SS101. Collectively these results suggest that sulfur assimilation in *Pf* SS101 has a neutral to negative effect on growth depending on the cultivar. In the Broccoli shoot metabolome, *Pf* SS101 enhanced defense-associated metabolites mainly from the phenylpropanoid pathway such as flavonols including kaempferol and quercetin glycosides, various hydroxycinnamates such as caffeic acid and ferulic acid as well as antioxidants such as ascorbic acid and the indole glucosinolate glucobrassicin, indolylmethyl-desulfoglucosinolate (desulfoglucobrassicin) and 4-methoxy-3-indolylmethyl glucosinolate (4-methoxyglucobrassicin). By contrast, the levels of flavonoids, hydroxycinnamates and the indole glucosinolates showed slight to moderate increases in seedlings treated with the mutant 20H12. The enhanced level of glucobrassicin and its derivatives in *Pf* SS101-treated seedlings suggests that sulfur assimilation in *Pf* SS101 might gear tryptophan metabolism in Broccoli towards the biosynthesis of indolic glucosinolates instead of the growth-promoting phytohormone IAA. Furthermore, the high abundance of flavonoids particularly the flavonol subclass in plants treated with *Pf* SS101 might impact auxin biosynthesis, transport (Besseau *et al.*, 2007), distribution and its conjugation/degradation (Kuhn *et al.*, 2016) thereby affecting plant growth. Additionally, the higher accumulation of phenylpropanoids and other carbon and energy costly secondary metabolites in Broccoli seedlings treated with *Pf* SS101 could pose resource limitation to plant growth-related processes and lead to an adverse effect on plant growth.

Although sulfur assimilation by *Pf* SS101 adversely affected overall growth in Broccoli, it

led to enhanced defense against *Xca* in a Broccoli cultivar-specific manner. When cultivar Coronado was treated on the roots with *Pf* SS101 and challenged on the leaves with *Xca,* a significantly reduced disease severity was observed while root treatment with mutant 20H12 was not effective. By contrast, both *Pf* SS101 and mutant 20H12 reduced disease severity caused by *Xca* in cultivar Malibu. The extent of *Pf* SS101-mediated changes in the Broccoli shoot metabolome, particularly towards defensive secondary metabolites such as flavonoids, hydroxycinnamates, lignin, iridoid glycosides and indolic glucosinolates was substantial. These classes of metabolites significantly increased in the shoots of both Broccoli cultivars upon root tip treatment with *Pf* SS101. Moreover, cultivar Malibu treated with mutant 20H12 also showed higher levels of these classes of metabolites, while in cultivar Coronado the level of these metabolites remained unchanged or showed reduced increase. Phenolic compounds can have direct or indirect inhibitory effect on bacterial pathogens. The direct effect involves disruption of growth- and reproduction-related processes in the pathogens (Maddox *et al.*, 2010; Xie, Y *et al.*, 2015), while the indirect effect involves limiting the pathogen ingress by fortifying the plant cell wall (Reimers & Leach, 1991; Miedes *et al.*, 2014). Similarly, the indolic glucosinolate glucobrassicin was reported to have inhibitory activity against *Xcc* in *Brassica oleracea* (Madloo *et al.*, 2019) and 4-methoxyglucobrassicin was implicated as a signal molecule in plant defense against bacteria and fungi (Bednarek *et al.*, 2009). Hence, *Pf* SS101-mediated systemic resistance in Broccoli against *Xca* and to some extent against *Xcc* is likely related, at least in part, to the observed changes in these shoot secondary metabolites. In conclusion, our result showed that sulfur assimilation in *Pf* SS101 can affect its interaction with the host and exhibit growth-promoting or growth-retarding effects in a plant species- and even cultivar-dependent manner. Furthermore, sulfur assimilation by *Pf* SS101 had significant impact on both sulfur-containing and non-sulfur containing metabolites such as glucosinolates and phenylpropanoids, respectively. These changes in the shoot metabolome are likely associated with pathogen defense and their impact is dependent on the pathovar (*Xca/Xcc*) of the pathogen.

Interestingly, there were other metabolite changes observed in Broccoli shoots that appear to be disconnected from sulfur assimilation in *Pf* SS101. For example, the level of ascorbic acid (vitamin C), an antioxidant element (Foyer, 2017; Smirnoff, 2018), was enhanced in *Pf* SS101-treated seedlings, suggesting an upregulation of the l-galactose pathway of ascorbate synthesis. In addition, a significant increase of scopolin, a coumarin glycoside, was detected in our study. Recent work on Arabidopsis treated with growth-promoting *Pseudomonas simiae* strain WCS417 revealed enhanced levels of scopoletin in root exudates (Stringlis et al. 2018). They further showed that scopoletin is an iron-mobilizing phenolic compound with selective antimicrobial activity that shapes the root-associated microbial community (Stringlis, Ioannis A *et al.*, 2018). Our results show that scopolin accumulates also in the leaves. If these coumarins also have antibacterial activity against leaf pathogenic *Pseudomonas syringae* tested in our previous study or against the two *Xanthomonas campestris* pathovars of Broccoli tested in this study will be subject of future investigations to unravel the importance of coumarins in

the observed ISR response. Integration of metabolomics with transcriptomics followed by targeted gene editing of pathways in the host plant will be needed to validate the functional importance of several of the metabolome changes observed in the shoots of Arabidopsis and other plant species following treatment with growth-promoting rhizobacteria.

Acknowledgements

Seeds of two Broccoli cultivars (*Brassica olearacea* var. italic), Coronado and Malibu, together with Broccoli leaf pathogen *Xanthomonas* spp. were kindly provided by Bejo seed company (Trambaan1, 1749 CZ Warmenhuizen, The Netherlands). We are grateful to Bert Schipper and Henriëtte Vaneekelen for their help with LC MS analysis and pre-processing of metabolomics data.

Supplementary materials

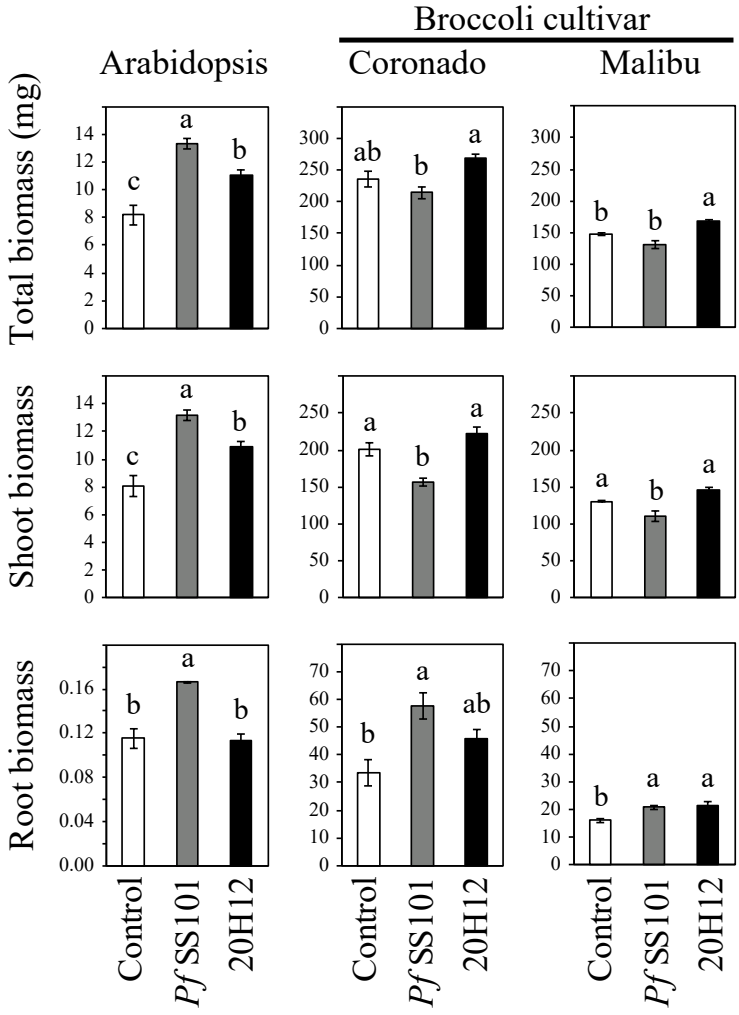

Fig S1. Biomass changes (absolute) of the whole plant, shoot and root after rhizobacteria treatment (11 dpi). Bars with different letters are significantly different among treatments according to one-way ANOVA (Tukey, $P<0.05$). For each plant species, four independent biological replicates were used with 10 seedlings of Arabidopsis and 5 of Broccoli per replicate. *Pf* SS101: *Pseudomonas fluorescens* SS101, 20H12: *cysH* gene mutant of *Pf* SS101.

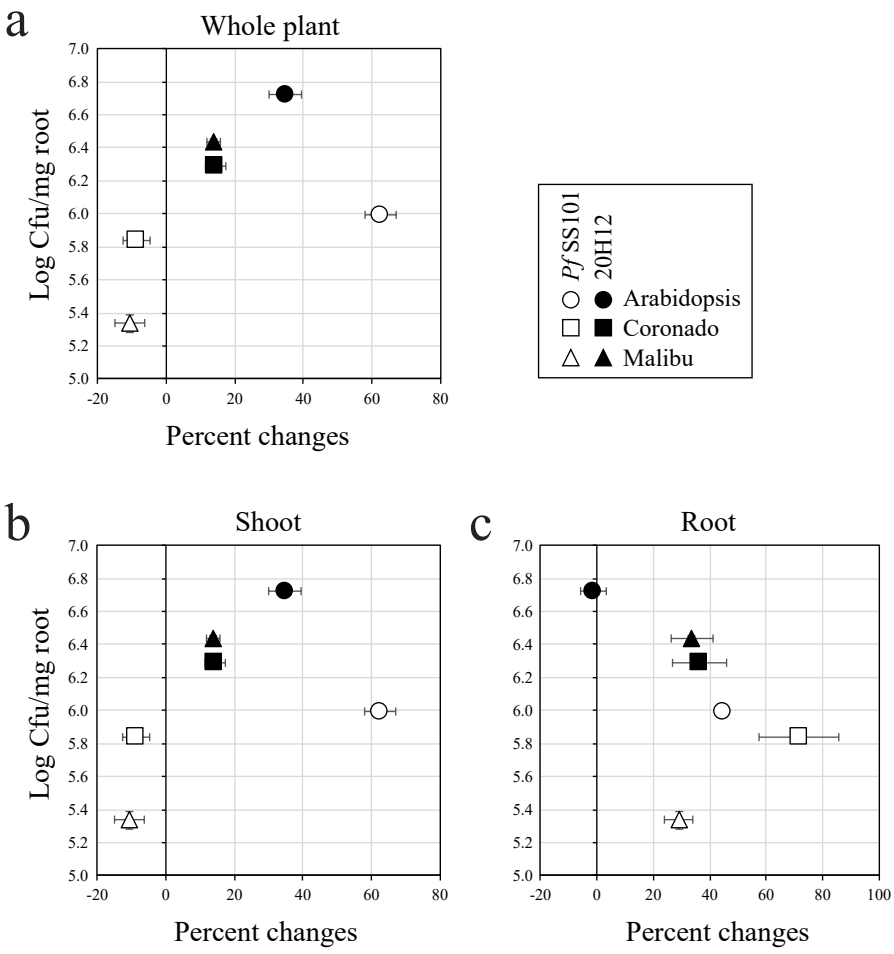

Fig S2. Correlation between host phenotypic changes and root colonization of *Pseudomonas fluorescens* SS101 and *cysH* mutant 20H12. Correlation between the rhizosphere population density of rhizobacteria (Log Cfu/mg root) and percent changes of biomass of whole plant (**a**), shoot (**b**) and root (**c**) of Arabidopsis and two Broccoli cultivars: Coronado and Malibu at 11dpi. *Pf* SS101: *Pseudomonas fluorescens* SS101, 20H12: *cysH* mutant of *Pf* SS101.

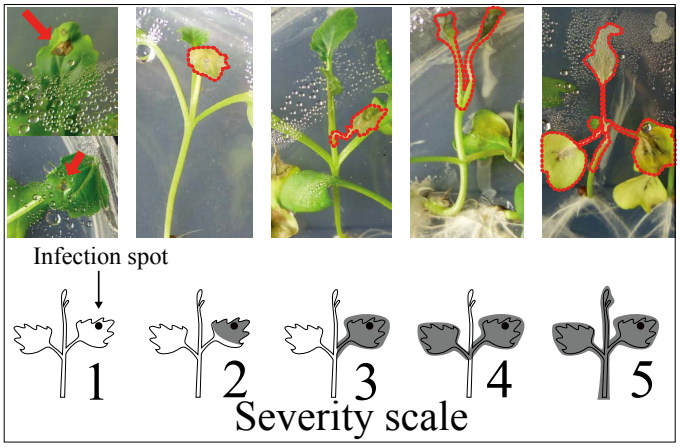

Fig S3. Disease severity scale used to assess the level of induced resistance in Broccoli at 11 dpi. 1 = no necrosis, no migration of the bacterial leaf pathogen *Xanthomonas campestris*, 2 = dispersal of the infection symptoms over the treated leaf, 3 = migration of the pathogen to the leafstalk of the treated leaf, 4 = migration to the neighboring leaf, and 5 = migration to the entire seedlings after infestation.

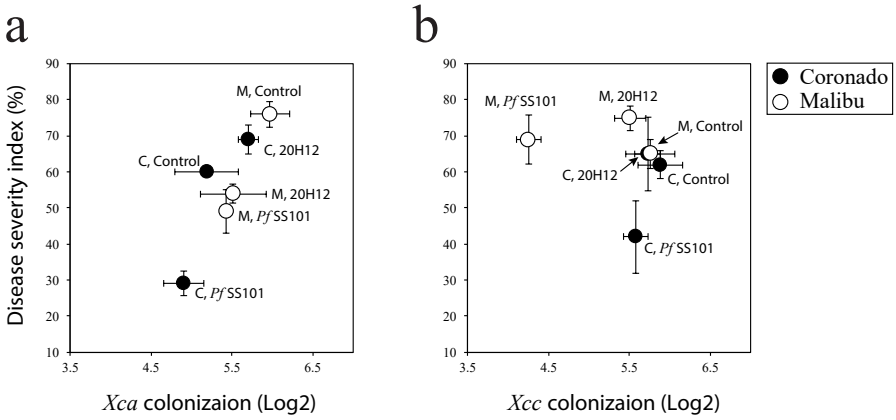

Fig S4. Correlation between disease severity of Broccoli and cell density of the bacterial pathogen *Xca* (**a**): *Xanthomonas campestris* pv. armoraciae, and *Xcc* (**b**): *Xanthomonas campestris* pv. campestris. C: Coronado, M: Malibu, Control: Broccoli without bacteria treatment, *Pf* SS101: *Pseudomonas fluorescens* SS101; 20H12: *cysH*-mutant of *Pf* SS101.

Table S1. Results of the analysis of variance ANOVA (type II) of phenotypic changes induced in tow Broccoli cultivars by root inoculation by *Pseudomonas fluorescens* strain SS101 or its *cysH* mutant 20H12. Shown are whole plant, shoot and root biomass changes in the two broccoli cultivars after root inoculation with *Pf* SS101: *Pseudomonas fluorescens* SS101, 20H12: *cysH*-mutant of *Pf* SS101.

Sample	Factor	Df	Sum Sq	Mean Sq	F value	Pr(>F)	
Whole plant fresh biomass relative change	Broccoli cultivars	2	11513	5757	94.559	2.83E-10	***
	Bacteria (WT vs Mutant)	1	260	260	4.263	0.0537	.
	Broccoli cultivars: Bacteria	2	3536	1768	29.043	2.32E-06	***
	Residuals	18	1096	61			
Shoot fresh biomass relative change	Broccoli cultivars	2	15124	7562	103.416	1.35E-10	***
	Bacteria	1	699	699	9.554	0.0063	**
	Broccoli cultivars: Bacteria	2	4373	2186	29.899	1.90E-06	***
	Residuals	18	1316	73			
Root fresh biomass relative change	Broccoli cultivars	2	4453	2226	8.477	0.00255	**
	Bacteria	1	3883	3883	14.783	0.00119	**
	Broccoli cultivars: Bacteria	2	2829	1415	5.386	0.01468	*
	Residuals	18	4728	263			

Significance codes: *** 0, ** 0.001, * 0.01. Bacteria (Wild type when compared to the mutant)

Table S2. Population density of *Pseudomonas fluorescens* SS101 and *cysH*-mutant 20H12 on roots of Arabidopsis and two Broccoli cultivars, Coronado and Malibu, at 11 dpi. *Pf* SS101: *Pseudomonas fluorescens* SS101, 20H12: *cysH*-mutant of *Pf* SS10*1*.

Plant species		Population density (Cfu/mg*)	
		***Pf* SS101**	**20H12**
Arabidopsis thaliana		$9.9 \pm 0.5 \times 10^5$	$5.3 \pm 0.3 \times 10^6$
Brassica oleracea var. italica	Coronado	$6.9 \pm 0.5 \times 10^5$	$2.0 \pm 0.1 \times 10^6$
	Malibu	$2.2 \pm 0.3 \times 10^5$	$2.7 \pm 0.1 \times 10^6$

CFU: Colony forming unit

*Values represent the average of 3 replicates ± SE of three replicates

Table S3. Effects of root treatment of two Broccoli cultivars with the beneficial rhizobacterium *Pseudomonas fluorescens* SS101, or with its *cysH*-mutant on the phylosphere population density of two pathovars of the bacterial leaf pathogen *Xanthomonas campestris* at 11 dpi. The two Broccoli cultivars are Coronado and Malibu; the two pathovars of *X. campestris* are *Xca*: *X. campestris* pv. armoraciae, and *Xcc*: *X. campestris* pv. campestris

Broccoli cultivars	Rhizobacteria pretreatments	Population density (Cfu/mg*)	
		Xca	*Xcc*
Coronado	Control	$4.4 \pm 3.3 \times 10^5$	$1.5 \pm 1.0 \times 10^6$
	Pf SS101	$1.2 \pm 0.6 \times 10^5$	$4.5 \pm 1.5 \times 10^5$
	20H12	$5.8 \pm 1.9 \times 10^5$	$6.4 \pm 2.1 \times 10^5$
Malibu	Control	$1.6 \pm 1.1 \times 10^6$	$1.1 \pm 6.2 \times 10^6$
	Pf SS101	$2.7 \pm 0.3 \times 10^5$	$2.1 \pm 0.1 \times 10^4$
	20H12	$8.5 \pm 5.4 \times 10^5$	$4.0 \pm 1.2 \times 10^5$

Cfu: Colony forming unit

*Values represent the average of 3 replicates ± SE of three replicates

Table S4. Results of the beta regression analysis of disease severity caused by *Xanthomonas* on leaves two Broccoli cultivars (Coronado and Malibu) that were pretreated on the roots with *Pseudomonas fluorescens* SS101 or its *cysH*-mutant.

Pathovar	model term	df1	df2	F.ratio	p.value
Xca	Rhizobacteria	2	Inf	43.681	<.0001
	Genotype	1	Inf	7.058	0.0079
	Rhizobacteria:Genotype	2	Inf	17.234	<.0001
Xcc	Rhizobacteria	2	Inf	2.878	0.0562
	Genotype	1	Inf	6.523	0.0106
	Rhizobacteria:Genotype	2	Inf	2.253	0.105

Table S5. Annotation of Arabidopsis shoot metabolites that showed significant change in their abundance after root inoculation with rhizobacterium *Pf* SS101: *Pseudomonas fluorescens* SS101, or its mutant 20H12: *cysH*-mutant of *Pf* SS101. Fold changes were calculated by dividing the abundance of each metabolite to the non-treated control. Cluster numbers are associated with the cluster in **Fig 3b.**

Cluster	RT(m)	Mass(D)	m/z	Compound	Formula	Δ ppm to data base	Classification	data base	Fold change	
									Pf SS101	20H12
1	19.9	388.0738	[M-H]-	Glucocleomin (2-Methylbutyl glucosinolate)	C12H23NO9S2	-0.78	Aliphatic GLS	KEGG	-2.09	-1.29
1	1.6	175.1189	[M-H]+	L-Arginine	C6H14N4O2	-0.46	Amino acid	KEGG	-2.15	-1.13
1	15.7	380.1559	[M-H]-	(R)-Pantothenic acid 4'-O-b-D-glucoside	C15H27NO10	-0.97	Fatty acyl glycoside	HMDB	-4.20	-1.55
1	11.3	222.0771	[M-H]-	N-Acetyl-L-tyrosine	C11H13NO4	-0.43	Tyrosine and derivative	HMDB	-3.25	-1.63
2	7.2	228.0501	[M-H]+	Stizolobic acid	C9H9NO6	-0.73	Amino acid	KEGG	-2.33	-1.68
2	1.9	145.0617	[M-H]-	L-Glutamine or (C05100)	C5H10N2O3	-1.12	Amino acid	KEGG	-2.27	-1.54
2	7.1	138.0559	[M-H]-	Gabaculine	C7H9NO2	-0.73	Benzoic acid	KEGG	-2.32	-1.63
2	27.7	395.191	[M-H]+	cis-3-Hexenyl b-primeveroside	C17H30O10	-0.34	Fatty acyl glycoside	HMDB	-3.70	-1.88
2	13.8	293.1241	[M-H]-	Ethyl (S)-3-hydroxybutyrate glucoside	C12H22O8	-0.26	Fatty acyl glycoside	HMDB	-2.42	-1.74
2	6.1	278.1234	[M-H]+	N-(1-Deoxy-1-fructosyl)proline	C11H19NO7	-0.16	Proline and	HMDB	-2.35	-1.61
2	3.0	130.05	[M-H]+	5-Oxoproline or (C01877), (C04282)	C5H7NO3	0.86		KEGG	-2.06	-1.66
2	37.0	591.1718	[M-H]-	Di-O-sinapoyl-beta-D-glucoside	C28H32O14	-0.29	Coumaric acid	KEGG	-2.17	-1.40
2	37.0	369.1178	[M+H]+	O-Feruloylquinic acid	C17H20O9	-0.48	Quinic acid	KEGG	-2.44	-1.45
3	3.9	450.0566	[M-H]-	Glucoalyssin (5-methylsulfinylpentyl glucosinolate)	C13H25O10S3N1	-0.41	Aliphatic GLS	KEGG	1.17	2.06
3	3.2	436.0409	[M-H]-	Glucoraphanin (4-Methylsulfinylbutyl glucosinolate)	C12H23O10S3N1	-0.46	Aliphatic GLS	KEGG	1.26	1.47
4	12.7	163.0754	[M+H]+	Methyl cinnamate	C10H10O2	0.11	Cinnamic acid derivative	KEGG	2.08	-1.36
4	14.9	355.1023	[M+H]+	Scopolin	C16H18O9	-0.23	Coumarin	KEGG	3.29	-1.37
4	14.9	399.0927	[M-H]-	Sinapinic acid-O-glucuronide isomer	C17H20O11	-1.59	hydroxycinnamic acid glycoside	HMDB	3.18	-1.45
4	12.7	387.1299	[M-H]-	Geniposide	C17H24O10	0.75	Iridoid	KEGG	2.14	-1.39
4	50.3	476.1084	[M-H]-	8-Methylthiooctyl glucosinolate (8MTO)	C16H31O9S3N1	-0.89	Aliphatic GLS	KEGG	2.12	1.31
4	23.3	187.1331	[M+H]+	3-Oxodecanoic acid	C10H18O3	1.24	Medium-chain keto acid	HMDB	16.49	3.07
5	20.4	492.1035	[M-H]-	Glucohirsutin (8-Methylsulfinyloctyl glucosinolate)	C16H31O10S3N1	-0.42	Aliphatic GLS	KEGG	4.48	3.49
5	42.5	201.0479	[M+H]+	Camalexin	C11H8N2S	2.17	Alkaloid	PubChem	20.51	17.31
5	44.0	176.0706	[M+H]+	Indole-3-acetic acid (IAA)	C10H9NO2	0.24	Alkaloid	KEGG	8.40	6.92
5	11.3	275.1513	[M-H]-	p-Coumaroylagmatine II	C14H20N4O2	0.05	Coumaric acid	KEGG	3.15	2.21
5	21.7	135.0451	[M-H]-	Phenylacetic acid	C8H8O2	-5.85	Phenylacetic acid	KEGG	2.21	2.81

Table S6. Annotation of Broccoli shoot metabolites that showed significant change in their abundance after root inoculation with rhizobacterium *Pf* SS101: *Pseudomonas fluorescens* SS101, or its mutant 20H12: *cysH*-mutant of *Pf* SS101. Fold changes were calculated by dividing the abundance of each metabolite to the non-treated control. Cluster numbers are associated with the cluster in **Fig 4b.**

Cluster number	RT (m)	Mass(D)	m/z	Compound	Formula	Δ ppm	Classification	data base	Fold change			
									Coronado		Malibu	
									Pf SS101	20H12	*Pf* SS101	20H12
1	1.8	154.062424	[M-H]-	Histidine	C6H9N3O2	-2.9	Amino acid	KEGG, Metlin	-2.1	-1.5	-2.0	-1.3
1	1.6	175.119202	[M+H]+	Arginine	C6H14N4O2	1.3	Amino acid	KEGG	-2.3	-1.4	-2.0	-1.3
1	3.0	188.056656	[M-H]-	N-Acetyl-L-glutamic acid	C7H11NO5	-2.2	Glutamic acid	KEGG	-3.9	-2.3	-3.0	-1.9
1	2.2	175.047012	[M-H]-	Allantoic acid	C4H8N4O4	-1.8	Alpha amino acid	KEGG	-4.7	-2.0	-3.0	-1.8
1	2.1	351.10257	[M-H]-	Benzylpenicilloic acid	C16H20N2O5S	1.6	Penicilloic acid	KEGG	-3.6	-2.6	-3.3	-2.2
1	3.2	152.986389	[M-H]-	3-Sulfolactaldehyde	C3H6O5S	0.4	Sulfuric acid	KEGG	-8.2	-4.5	-8.0	-3.1
2	3.1	166.086502	[M+H]+	Phenylalanine	C9H11NO2	0.8	Amino acid	KEGG	-1.5	-1.7	-1.5	-2.1
2	6.5	205.097321	[M+H]+	Tryptophan	C11H12N2O2	0.7	Amino acid	KEGG	-2.3	-3.2	-1.8	-3.8
2	43.2	631.276428	[M+H]+	Brassica napus non-fluorescent chlorophyll catabolite 3	C34H38N4O8	0.3	Tetrapyrrole	HMDB	-4.4	-3.8	-1.9	-2.2
4	15.8	193.049622	[M+H]+	Scopoletin or (C18079)	C10H8O4	0.2	Coumarin	KEGG	-8.9	2.1	19.4	6.5
5	5.8	298.096924	[M+H]+	Methylthioadenosine	C11H15N5O3S	0.2	Thionucleoside	KEGG	2.1	1.5	1.7	1.2
5	2.0	132.03035	[M-H]-	Aspartic acid	C4H7NO4	-2.8	Amino acid	KEGG	3.5	2.1	2.6	2.1
5	17.8	278.067352	[M-H]-	N-[4'-hydroxy-(E)-cinnamoyl]-L-aspartic acid	C13H13NO6	1.2	Aspartic acid	HMDB	3.3	1.9	2.3	1.4
5	13.5	299.077423	[M-H]-	4-(beta-D-Glucosyloxy)benzoate	C13H16O8	0.7	Benzoic acid	KEGG	40.0	1.6	5.0	-1.4
5	2.2	175.025177	[M-H]-	Ascorbic acid	C6H8O6	-1.2	Butenolide	KEGG	2.7	2.4	2.3	2.2
5	2.2	177.039734	[M+H]+	Ascorbic acid	C6H8O6	2.0	Butenolide	KEGG	4.5	3.6	2.5	2.2
5	4.3	173.009323	[M-H]-	Dehydroascorbic acid	C6H6O6	-3.1	Butenolide	KEGG	3.4	2.0	2.5	1.8
5	17.9	385.11441	[M-H]-	1-O-Sinapoyl beta-D-glucoside	C17H22O10	1.0	Coumaric acid	KEGG	3.7	1.6	2.1	1.2
5	17.2	355.102661	[M+H]+	Scopolin or (C00852) or (C08996)	C16H18O9	0.8	Coumarin	KEGG	3.1	1.5	2.3	1.4
5	33.3	577.15686	[M-H]-	Daidzein 4',7-diglucoside	C27H30O14	1.0	Flavonoid	HMDB	5.2	2.1	2.9	1.5
5	35.4	723.21521	[M-H]-	Flavonol 3-O-beta-D-glucosyl-(1->2)-beta-D-glucosyl-(1->2)-beta-D-glucoside	C33H40O18	1.4	Flavonoid	KEGG	4.3	2.1	2.7	1.5
5	20.8	947.247437	[M-H]-	Kaempferol 3-(2-feruloylsophoroside) 7-glucoside	C43H48O24	1.2	Flavonoid	HMDB	2.4	1.2	2.3	1.3
5	20.3	611.160583	[M+H]+	Kaempferol 3-O-beta-D-sophoroside or (C05625), (C17563)	C27H30O16	-0.2	Flavonoid	KEGG	3.7	1.7	2.6	1.5
5	18.0	935.245972	[M+H]+	Kaempferol 3-O-caffeoyl-sophoroside 7-O-glucoside or (HMDB0037938)	C42H46O24	0.8	Flavonoid	HMDB	2.1	1.2	3.0	1.7
5	20.8	949.261597	[M+H]+	Kaempferol 3-sophoroside 7-(2-feruloylglucoside) or (HMDB0040801), (HMDB0029269)	C43H48O24	0.8	Flavonoid	HMDB	2.3	1.2	2.7	1.4
5	30.5	739.210815	[M-H]-	Mauritianin	C33H40O19	2.3	Flavonoid	HMDB	3.4	1.7	2.6	1.4
5	18.0	933.231323	[M-H]-	Quercetin 3-[p-coumaroyl-(->6)-glucosyl-(1->2)-glucosyl-(1->2)-glucoside]	C42H46O24	0.7	Flavonoid	HMDB	2.3	1.2	3.2	1.8
5	30.1	739.210693	[M-H]-	Robinin	C33H40O19	2.1	Flavonoid	KEGG	5.4	2.5	3.0	1.5
5	20.3	609.146667	[M-H]-	Rutin	C27H30O16	0.9	Flavonoid	KEGG	3.4	1.5	3.0	1.6
5	28.9	665.173584	[M-H]-	Sudachiin B or (HMDB39088)	C30H34O17	1.9	Flavonoid	HMDB	5.0	2.0	5.3	2.2
5	38.8	561.162048	[M-H]-	Flavonol 3-O-beta-D-glucosyl-(1->2)-beta-D-glucoside	C27H30O13	1.3	Flavonoid	KEGG	10.3	4.0	5.4	2.5

Table S6. (Continued)

Cluster number	RT (m)	Mass(D)	m/z	Compound	Formula	Δ ppm	Classification	data base	Fold change			
									Coronado		Malibu	
									Pf SS101	20H12	*Pf* SS101	20H12
5	14.6	773.213074	[M+H]+	Kaempferol 3-sophorotrioside	C33H40O21	-0.5	Flavonoid	KEGG	2.3	1.1	1.7	1.2
5	33.9	547.146606	[M-H]-	Puerarin xyloside	C26H28O13	1.6	Flavonoid	KEGG	12.8	3.5	6.3	2.6
5	2.2	289.033173	[M-H]-	Sedoheptulose phosphate or (C19882)	C7H15O10P	0.5	Hexose phosphate	KEGG	4.1	2.0	3.9	1.6
5	40.0	929.27356	[M-H]-	2-Feruloyl-1,2'-disinapoylgentiobiose	C44H50O22	1.6	Hydroxycinnamate	HMDB	2.6	1.3	2.2	1.4
5	19.8	355.103882	[M-H]-	1-O-Feruloyl-beta-D-glucose	C16H20O9	-0.4	Hydroxycinnamate	KEGG	3.2	1.6	1.8	1.4
5	11.4	181.049728	[M+H]+	Caffeic acid	C9H8O4	0.8	Hydroxycinnamate	KEGG	3.2	2.0	2.0	1.7
5	11.4	341.088074	[M-H]-	Caffeic acid 3-glucoside or (C10433)	C15H18O9	0.7	Hydroxycinnamate	KEGG	2.9	1.9	2.0	1.7
5	18.7	195.065338	[M+H]+	Ferulic acid	C10H10O4	0.8	Hydroxycinnamate	KEGG	3.2	1.7	1.8	1.4
5	19.9	195.065308	[M+H]+	Ferulic acid	C10H10O4	0.7	Hydroxycinnamate	KEGG	2.2	1.6	1.4	1.5
5	16.7	225.075836	[M+H]+	Sinapic acid	C11H12O5	0.3	Hydroxycinnamate	KEGG	2.0	1.2	1.8	1.2
5	27.8	477.064667	[M-H]-	4-Methoxyglucobrassicin (4-Methoxy-3-indolylmethyl glucosinolate)	C17H22N2O10S2	0.7	Indolic GLS	KEGG	2.3	-1.1	1.7	-1.0
5	21.7	369.11145	[M+H]+	Desulfoglucobrassicin (Indolylmethyl-desulfoglucosinolate)	C16H20N2O6S	-0.1	indolic GLS	KEGG	3.9	1.8	3.3	1.9
5	21.7	447.054474	[M-H]-	Glucobrassicin (3-Indolylmethylglucosinolate)	C16H20O9S2N2	1.7	Indolic GLS	KEGG	5.1	1.9	3.8	2.0
5	34.5	477.064697	[M-H]-	neoglucobrassicin (1-Methoxy-3-indolylmethyl glucosinolate)	C17H22O10S2N2	0.8	Indolic GLS	KEGG	3.5	1.2	3.6	1.5
5	36.2	693.204773	[M-H]-	Sesaminol glucosyl-(1->2)-glucoside	C32H38O17	1.7	Lignan	HMDB	4.2	1.8	3.7	1.7
5	37.4	693.204773	[M-H]-	Neocuscutoside C	C32H38O17	0.7	Lignan glycoside	Metlin MS	5.9	2.1	4.4	2.0
5	4.5	315.072632	[M-H]-	Ginnalin B	C13H16O9	-0.7	Phenolic glycoside	Metlin MS	7.2	1.2	4.3	1.1
5	26.6	415.125183	[M-H]-	2-Hydroxybenzaldehyde O-[xylosyl-(1->6)-glucoside]	C18H24O11	1.4	Phenolic glycoside	HMDB	5.7	2.0	2.7	1.7
5	13.0	371.098541	[M-H]-	Dihydroferulic acid 4-O-glucuronide	C16H20O10	0.5	Phenolic glycoside	HMDB	4.7	1.9	3.8	2.0
5	38.9	339.107605	[M+H]+	Hydrojuglone glucoside	C16H18O8	0.5	Phenolic glycoside	HMDB	8.8	3.7	5.3	2.6
5	10.2	355.102448	[M+H]+	Chlorogenic acid	C16H18O9	0.2	Quinic acid	KEGG	3.9	1.9	2.3	1.4
5	37.9	369.118317	[M+H]+	O-Feruloylquinic acid I	C17H20O9	0.9	Quinic acid	KEGG	2.2	1.2	1.5	1.2
5	17.6	367.103668	[M-H]-	O-Feruloylquinic acid II	C17H20O9	-0.7	Quinic acid	KEGG	2.1	1.3	1.4	1.1
5	33.1	577.156799	[M-H]-	Glucofrangulin A	C27H30O14	0.8	Quinone	KEGG	3.2	-5.6	1.6	1.9
5	18.7	355.103821	[M-H]-	Gentiopicroside	C16H20O9	1.1	Secoiridoid	KEGG	3.5	1.7	1.9	1.3
5	34.1	469.081787	[M-H]-	(Z)-Resveratrol 3-(3''-sulfoglucoside) or (HMDB37073), (HMDB37076)	C20H22O11S	1.7	Stilbene	HMDB	2.8	2.0	2.3	1.7
5	2.1	195.050842	[M-H]-	D-Gluconic acid	C6H12O7	-0.9	Sugar acid	KEGG	3.2	1.7	2.1	1.5
5	3.0	191.019897	[M-H]-	Citric acid	C6H8O7	-2.4	Tricarboxylic acid	KEGG, Metlin	2.9	2.4	3.1	2.3
5	35.4	501.160126	[M+H]+	Nocardicin A	C23H24N4O9	-4.4		KEGG	4.6	2.2	2.9	1.6
7	14.9	339.107605	[M+H]+	p-Coumaroyl quinic acid or (C10432), (C10441)	C16H18O8	0.4	Quinic acid	KEGG	3.9	1.8	2.1	1.3
7	2.8	133.014282	[M-H]-	Malic acid	C4H6O5	-4.4	Hydroxy acid	KEGG, Metlin	2.0	2.3	2.5	2.0
10	24.1	306.097595	[M+H]+	Ascorbigen	C15H15NO6	1.2	Isosorbide	HMDB	7.1	2.7	6.5	2.7
11	12.1	406.031067	[M-H]-	Glucoiberverin (3-Methylthiopropyl glucosinolate)	C11H21NO9S3	1.3	Aliphatic GLS	KEGG	2.3	1.0	1.3	3.1

Table S6. (Continued)

Cluster number	RT (m)	Mass(D)	m/z	Compound	Formula	Δ ppm	Classification	data base	Fold change			
									Coronado		Malibu	
									Pf SS101	20H12	*Pf* SS101	20H12
11	34.4	191.14299	[M+H]+	beta-Damascenone	C13H18O	-0.3	Enone	HMDB	2.6	1.1	1.5	-1.4
12	16.2	165.054794	[M+H]+	p-Coumaric acid or (C00166), (C12621), (C01772)	C9H8O3	1.3	Hydroxycinnamate	KEGG	2.3	1.7	1.2	1.2
12	16.2	325.093597	[M-H]-	4-O-beta-D-Glucosyl-4-hydroxycinnamate or (C16827), (C05158)	C15H18O8	0.1	Hydroxycinnamate	KEGG	2.9	1.7	-1.1	1.1
12	2.2	209.066757	[M-H]-	Coriose or (C21043), (C02076)	C7H14O7	-2.9	Glycoside	KEGG	2.2	1.7	1.6	1.6
12	2.3	110.985336	[M-H]-	Hydroxymethylphosphonate	CH5O4P	-3.5	Phosphonic acid	KEGG	3.0	1.7	2.0	2.2
13	3.9	173.009308	[M-H]-	trans-Aconitic acid or (C05422)	C6H6O6	-3.2	Tricarboxylic acid	HMDB	2.1	3.7	2.4	1.7